

A new two-dimensional donor/acceptor copolymer based on 4,8-bis(2'-ethylhexylthiophene)thieno [2,3-*f*]benzofuran for high-performance polymer solar cells†

Cite this: *J. Mater. Chem. C*, 2014, 2, 5651

Ling Fan,^{‡a} Ruili Cui,^{‡ab} Xiuping Guo,^{‡a} Dong Qian,^a Beibei Qiu,^a Jun Yuan,^a Yongfang Li,^b Wenlong Huang,^c Junliang Yang,^c Weifang Liu,^a Xinjun Xu,^d Lidong Li^d and Yingping Zou^{*abe}

A new alkylthienyl substituted thieno[2,3-*f*]benzofuran (TBF)-based polymer (PTBFTDTBT) was synthesized and characterized. PTBFTDTBT had a high molecular weight, good solubility in common organic solvents, broad visible absorption from 300 to 750 nm, and a relatively deep highest occupied molecular orbital level (−5.2 eV). PTBFTDTBT also showed a field hole mobility up to the order of 10^{-2} using an organic field effect transistor (OFET) method and an order of 10^{-2} using a space-charge-limited current (SCLC) method. With the structure of indium tin oxide (ITO)/poly(3,4-ethylenedioxythiophene):polystyrene sulfonate/PTBFTDTBT:PC₇₁BM (1 : 2, w/w)/Ca/Al, a power conversion efficiency of 6.42% was obtained with a high short circuit current (J_{sc}) of 13.51 mA cm^{−2} and fill factor (FF) of 61%, under the illumination of AM1.5G, at 100 mW cm^{−2}, without any post-treatment. The study demonstrates that TBF is a promising building block for organic electronics.

Received 13th April 2014

Accepted 21st May 2014

DOI: 10.1039/c4tc00738g

www.rsc.org/MaterialsC

1. Introduction

Polymer solar cells (PSC) offer many advantages for photovoltaic applications, including flexibility, low-cost and roll-to-roll fabrication.¹ Significant progress in PSC has been achieved in the past decade by the development of new polymers and device processing. To date, power conversion efficiencies (PCE) have reached 10.6% using a tandem bulk hetero junction (BHJ) structure,² indicating that PSC have great potential for future energy generation. The BHJ device architecture includes an active layer of a p-type conjugated polymer electron donor and an n-type fullerene derivative electron acceptor.³

The structural design of new solution-processable polymer donor materials plays an important role in the development of PSC. In the past decade, two-dimensional (2D) conjugated polymers with conjugated side chains have been introduced into PSC to improve the performance.⁴ The widely investigated 2D conjugated block was the alkylthienyl-substituted benzodichalcogenophene (BDC) unit, because a 2D conjugated BDC unit usually possesses a lower highest occupied molecular orbital (HOMO) level and stronger absorption than an alkoxy-substituted BDC unit, which are beneficial for obtaining high open-circuit voltage (V_{oc}) and short circuit current (J_{sc}).⁵ Huo *et al.*, have synthesized several alkylthienyl-substituted BDC-based polymers; for example, PCE of benzodifuran (BDF)-based polymer (PBDFTT-CF-T) and benzodithiophene (BDT)-based polymer (PBDTTT-C-T) reached 6.26% and 7.6%, respectively, when 3% of 1,8-diiodooctane (DIO) was used as a processing additive.^{3d,6} Our group have also reported a BDF-based polymer with a PCE up to 6.0% without any post-treatment.⁷ Combining the advantages of the BDT and BDF units, the thiophene ring in the BDT unit was replaced with a furan ring, and therefore, a new donor building block: thieno[2,3-*f*]benzofuran (TBF)⁸ was envisaged. Interestingly, TBF is a non-symmetric building block, just like thieno[3,4-*b*]thiophene (TT)⁹ unit. TT-based regiorandom polymers show promising photovoltaic properties; for example, TT-based polymer – PTB7 – has reached a high PCE of up to 9.2% using PFN as the interface modifier.¹⁰ A polymerization reaction with a non-symmetric monomer has a tendency to form high molecular weight copolymers.^{11a} Generally, a high molecular weight is beneficial to improving J_{sc} .^{11b}

^aCollege of Chemistry and Chemical Engineering, Central South University, Changsha 410083, China. E-mail: yingpingzou@csu.edu.cn

^bInstitute of Super-microstructure and Ultrafast Process in Advanced Materials, School of Physics and Electronics, Central South University, Changsha, Hunan 410083, China

^cBeijing National Laboratory for Molecular Sciences, Institute of Chemistry, Chinese Academy of Sciences, Beijing 100190, China

^dSchool of Materials Science and Engineering, University of Science and Technology, Beijing, Beijing 100083, China

^eState key Laboratory for Powder Metallurgy, Central South University, Changsha 410083, China

† Electronic supplementary information (ESI) available: ¹H-NMR of compound 4, ¹H-NMR of the monomer M1, ¹³C-NMR of the monomer M1 and ¹H-NMR of PTBFTDTBT are shown in Fig. S1–S4. FET curves are shown in Fig. S5, TEM images of PTBFTDTBT and PCBM blends are shown in Fig. S6. See DOI: 10.1039/c4tc00738g

‡ L. Fan, R. Cui and X. Guo contributed equally to this work.

Based on the above considerations, we designed and synthesized a new TBF-based 2D-conjugated polymer, poly{4,8-bis(2'-ethylhexylthiophene)thieno[2,3-*f*]benzofuran-*alt*-5,5-(4',7'-di-2-thienyl-5',6'-dioctyloxy-2',1',3'-benzothiadiazole)} (PTBFTDTBT, shown in Scheme 1). The properties of PTBFTDTBT including the absorption, energy levels, charge transporting, blend film morphologies and photovoltaic properties, have been well investigated and discussed. PTBFTDTBT showed a low bandgap and a moderately high hole mobility. Using the device structure of indium tin oxide (ITO)/poly(3,4-ethylenedioxythiophene): polystyrene sulfonate (PEDOT:PSS)/PTBFTDTBT:phenyl C₇₁ butyric acid methyl ester (PC₇₁BM) (1 : 2, w/w)/Ca/Al, PTBFTDTBT displayed a promising PCE of 6.42% with a high J_{sc} of 13.51 mA cm⁻² under illumination of AM1.5G (100 mW cm⁻²) without any post-treatment. Device performance of PTBFTDTBT (PCE = 6.4%) is much higher than PBDTDTBT (PCE = 4.9%).¹² The preliminary results demonstrate that TBF-based polymers are probably promising donor materials for high performance PSC.

2. Experimental section

2.1 Materials

n-Butyl lithium (*n*-BuLi), Pd(PPh₃)₄, Sn(CH₃)₃Cl and thiophene-3-carbaldehyde were obtained from Aladdin and Alfa Asia Chemical Co., and they were used as received without further

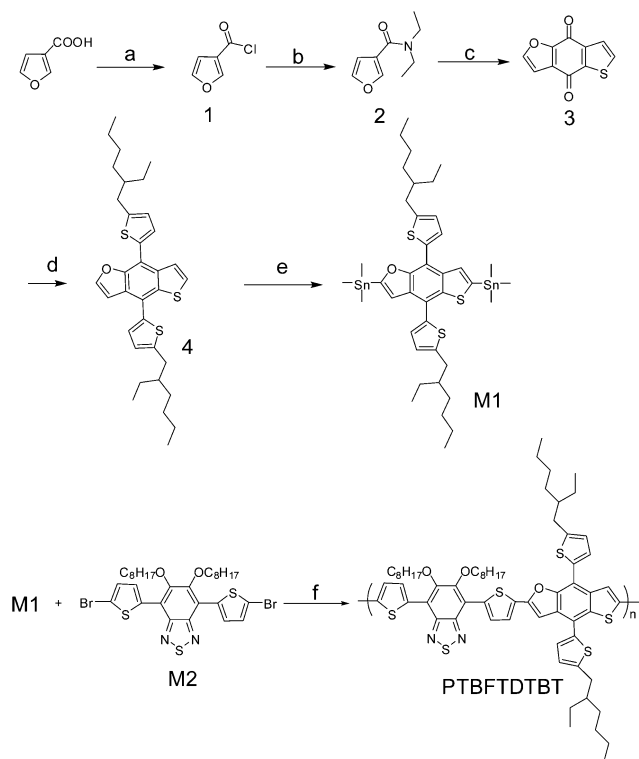
purification. Tetrahydrofuran (THF) and toluene were dried over Na/benzophenoneketyl and freshly distilled prior to use. Other reagents and solvents were purchased commercially as ACS-grade quality and used without further purification. 2-(2-Ethylhexyl)thiophene^{4a} and 4,7-di(5-bromo-thiophen-2-yl)-5,6-dioctyloxybenzo[*c*][1,2,5]-thiadiazole (M2)¹³ were prepared according to previously reported procedures. All other compounds were synthesized following the procedures described here.

2.2 Characterization

Nuclear magnetic resonance (NMR) spectra were recorded using a Bruker DMX-400 spectrometer in deuterated chloroform (CDCl₃) solution at 298 K, unless specified otherwise. Chemical shifts were reported as δ values (ppm) relative to an internal tetramethylsilane (TMS) standard. Number-average (M_n) and weight-average (M_w) molecular weights were measured by gel permeation chromatography (GPC) analysis with polystyrene as a standard and THF (HPLC grade) as the eluent at a flow rate of 1.0 mL min⁻¹ at 35 °C. Thermogravimetric analysis (TGA) was performed on a Perkin-Elmer TGA-7 at a heating rate of 10 K min⁻¹ under a nitrogen atmosphere. UV-Vis absorption spectra were recorded using a Hitachi U-3010 UV-Vis spectrophotometer. For solid state measurements, a polymer solution in chloroform was cast on a quartz plate. The optical bandgap was calculated from the onset of the absorption band. Cyclic voltammograms (CV) were recorded on a Zahner IM6e Electrochemical Workstation (Germany) with a three-electrode system in a solution of 0.1 M Bu₄NPF₆ in acetonitrile at a scan rate of 50 mV s⁻¹. The polymer films were transferred on to a glassy carbon electrode (1.0 cm²) by dipping the corresponding solutions in the electrode, with a platinum wire as the counter electrode and Ag/AgCl as the reference electrode. The HOMO energy level was determined from the oxidation onset from the CV curve. Electrochemical onset was determined at the position where the current starts to differ from the baseline. Hole field effect mobility of the polymer was measured by using an OFET method performed on a Keithley 4200 SCS semiconductor parameter analyzer. The morphologies of the polymer/PC₇₁BM blend films were investigated by atomic force microscopy (AFM; Agilent Technologies, 5500 AFM/SPM System, USA) with tapping-mode. Transmission electron microscope (TEM) measurements were performed in a JEM-2100F.

2.3 Fabrication and characterization of polymer solar cells

PSC were fabricated in the configuration of the traditional sandwich structure with an ITO glass positive electrode and a metal negative electrode. A patterned ITO glass with a sheet resistance of 10 $\Omega \square^{-1}$ was purchased from CSG HOLDING Co. LTD. (China). The ITO glass was cleaned by sequential ultrasonic treatments in detergent, deionized water, acetone and isopropanol and then the glass was treated in an ultraviolet-ozone chamber (Ultraviolet Ozone Cleaner, Jelight Company, USA) for 20 min. The PEDOT:PSS (Baytron P 4083, Germany) was used as anode buffer layer to smooth the ITO surface, and was filtered through a 0.45 μ m poly(vinylidene fluoride) filter



Scheme 1 Synthesis and molecular structures of the monomer and polymer. Reagents and conditions: (a) SOCl₂, 70 °C, 100% yield; (b) diethylamine, CH₂Cl₂, 78% yield; (c) THF, *n*-BuLi, thiophene-3-carbaldehyde, 46% yield; (d) THF, *n*-BuLi, 2-(2-ethylhexyl)thiophene, SnCl₂·2H₂O, -78 °C, 41% yield; (e) THF, *n*-BuLi, Sn(CH₃)₃Cl, -78 °C, 80% yield; (f) toluene, dimethylformamide, Pd(PPh₃)₄, 110 °C, 81% yield.

and drop-coated at 3000 rpm for 40 s on the cleaned ITO electrode. Subsequently, the PEDOT:PSS film was baked at 150 °C for 15 min in air to give a thin film. A blend of the polymer and phenyl butyric acid methyl ester (PCBM) (different weight ratios, 10 mg mL⁻¹ for polymer) was dissolved in *o*-dichlorobenzene (ODCB), and spin-cast at 1700 rpm for 90 s onto the PEDOT:PSS layer. A bilayer cathode consisting of Ca (~20 nm) capped with Al (~40 nm) was thermally evaporated under a shadow mask with a base pressure of *ca.* 10⁻⁵ Pa. The active area of the PSC is 4 mm². *J-V* curves were recorded with a computer-controlled Keithley 236 digital source meter. A xenon lamp with an AM1.5G filter was used as a white-light source and the optical power was 100 mW cm⁻². All the fabrication and characterizations after the cleaning of the ITO substrates were performed in a glove box.

2.4 Fabrication of OFET devices

Thin-film OFETs were fabricated with a bottom-gate/top-contact configuration. Heavily p⁺ doped silicon wafer substrates (Si-Mat, Germany) covered with a thermally grown 300 nm SiO₂ layer were used as the gate, of which the capacitance was 10 nF cm⁻². The substrates were sequentially cleaned with detergent, deionized water, acetone and ethanol in an ultrasonic bath for 15 min each. Subsequently, hydrophilic treatment of these silicon wafers was performed according to the standard procedure. Briefly, the substrates were soaked in a mixture of deionized water, 25% ammonium hydroxide and 30% H₂O₂ (5 : 1 : 1 by volumetric ratio) for 20 min at 80 °C, then rinsed with deionized water and dried under a nitrogen flow. An octadecyltrichlorosilane (OTS) self-assembled monolayer was deposited and selected as a dielectric modification layer. Thin polymer films were prepared by spin coating of PTBFTDTBT (8 mg mL⁻¹) in ODCB onto the OTS modified substrates at a speed of 2000 rpm (revolutions per minute) for 50 s at room temperature. With or without annealing at 150 °C under atmosphere for 10 min, gold film (50 nm) was deposited on the organic layer to form the drain and source electrodes, for a typical device. The drain-source channel length (*L*) and width (*W*) were 80 μm and 1000 μm, respectively. OFET measurements were performed at room temperature using a Keithley 4200 SCS semiconductor parameter analyzer under ambient conditions.

2.4 Synthesis of the monomer and polymer

Furan-3-carbonyl chloride (1). 3-Furoic acid (25.1 g, 0.224 mol) and thionyl chloride (SOCl₂) (65.3 mL, 0.9 mol) were put into a dry three-necked round bottomed flask. The mixture was stirred at 70 °C for 4 h. It was then cooled to room temperature and the redundant solvent was removed under vacuum to give compound **1**, a brown oil, which was used in the next step without further purification.

***N,N*-diethylfuran-3-carboxamide (2).** Diethylamine (92.6 mL) and dichloromethane (100 mL) were mixed in a three-necked round-bottomed flask. Then, furan-3-carbonyl chloride (**1**) (29.24 g, 224 mmol) was added dropwise at 0 °C. The reaction mixture was warmed up to room temperature and stirred for 1 h. Then the reaction mixture was poured into 100 mL of ice-

water and the mixture was extracted with dichloromethane. The combined organic phases were dried over magnesium sulfate. After the solvents were evaporated under vacuum, the crude product was purified on a silica gel column with petroleum ether-ethyl acetate (1 : 2, v/v) as eluent, to give compound **2** as an orange-red oil (29.18 g, 78% yield).

¹H-NMR (CDCl₃, 400 MHz): δ: 7.70 (dd, *J* = 0.9, 1.5 Hz, 1H), 7.41 (dd, *J* = 1.5, 1.8 Hz, 1H), 6.59 (dd, *J* = 0.9, 1.8 Hz, 1H), 3.48 (q, *J* = 7.1 Hz, 4H), 1.21 (t, *J* = 7.1 Hz, 6H).

Thieno[2,3-*f*]benzofuran-4,8-dione (3).⁸ A solution of compound **2** (8.36 g, 50 mmol) in dry anhydrous THF (200 mL) was deoxygenated with argon for 15 min. Then the solution was cooled to -78 °C, *n*-BuLi (21.87 mL, 52.5 mmol) was added dropwise within 5 min. The reaction mixture was stirred for 15 min, and then freshly distilled thiophene-3-carboxaldehyde (5.88 g, 52.5 mmol) in THF (75 mL) was added dropwise within 15 min. The reaction mixture was stirred for another 2 h at -78 °C, and a solution of *n*-BuLi (21.87 mL, 52.5 mmol) was added to the reaction mixture. After that, the reaction mixture was warmed up to room temperature and stirred overnight. The reaction solution was poured into 200 mL water and extracted with CH₂Cl₂; then the extractions were concentrated by distillation under reduced pressure. After cooling, the solid precipitate was recrystallized in C₂H₅OH and after filtration gave compound **3** as a yellow solid (4.7 g, 46% yield).

¹H-NMR (400 MHz, CDCl₃): δ: 7.74 (d, *J* = 1.8 Hz, 1H), 7.71 (d, *J* = 5.0 Hz, 1H), 7.65 (d, *J* = 5.0 Hz, 1H), 6.97 (d, *J* = 1.8 Hz, 1H).

4,8-Bis(2'-ethylhexylthiophene)thieno[2,3-*f*]benzofuran (4). A solution of 2-(2-ethylhexyl)thiophene (3.92 g, 20 mmol) in dry anhydrous THF (5 mL) was deoxygenated with argon for 15 min. Then the mixture was cooled to 0 °C and *n*-BuLi (9 mL, 21.6 mmol) was added dropwise. After that, the reaction was refluxed for 1.5 hours at 50 °C. Then SnCl₂·2H₂O (14.5 g, 64 mmol) in 25.6 mL of 10% hydrogen chloride acid was added to the solution, and the mixture was vigorously stirred for an additional 1.5 hours. The reaction solution was then poured into water (100 mL), extracted with CH₂Cl₂, and sequentially washed with water, saturated aqueous NaHCO₃, aqueous 1 M Na₂SO₃ and water. After the solvent was removed under vacuum, the residue was purified by column chromatography (silica gel, PE) to give compound **4** as a pale yellow oil (1.85 g, 41% yield).

¹H-NMR (400 MHz, CDCl₃): δ: 7.92 (d, *J* = 5.7 Hz, 1H), 7.78 (d, *J* = 2.3 Hz, 1H), 7.51 (t, *J* = 5.3 Hz, 1H), 7.49-7.44 (m, 2H), 7.22 (d, *J* = 2.3 Hz, 1H), 6.92 (dd, *J* = 7.7, 4.7 Hz, 2H), 2.93-2.84 (m, 4H), 1.71 (dd, *J* = 11.9, 5.9 Hz, 2H), 1.53-1.27 (m, 16H), 1.04-0.87 (m, 12H).

2,6-Bis(trimethyltin)-4,8-bis(2'-ethylhexylthiophene)thieno[2,3-*f*]benzofuran (M1). A solution of compound **4** (1.126 g, 2 mmol) in dry anhydrous THF (5 mL) was deoxygenated with argon for 15 min. The mixture was cooled to -78 °C and *n*-BuLi (3.0 mL, 7.0 mmol) was added dropwise. The reaction mixture was stirred for 1 hour at -78 °C, then warmed to room temperature for 1 hour, and then cooled again to -78 °C; trimethyl tin chloride (8.0 mL, 8.0 mmol) was added, and the reaction mixture was allowed to warm up to room temperature and stirred overnight. After that, the mixture was poured into water (100 mL), extracted with CH₂Cl₂, and washed with water,

saturated aqueous NaHCO_3 and water. After the solvent was removed under vacuum, the residue was purified by recrystallization from isopropyl alcohol and dried under vacuum to obtain a pure compound, **M1**, as a pale yellow solid (1.4 g, 80% yield).

$^1\text{H-NMR}$ (400 MHz, CDCl_3): δ : 7.99 (d, $J = 15.2$ Hz, 1H), 7.55–7.50 (m, 1H), 7.48 (t, $J = 3.6$ Hz, 1H), 7.35–7.30 (m, 1H), 6.92 (dt, $J = 16.3, 8.2$ Hz, 2H), 2.90 (dd, $J = 11.0, 6.7$ Hz, 4H), 1.72 (dd, $J = 12.0, 6.0$ Hz, 2H), 1.55–1.21 (m, 16H), 1.07–0.85 (m, 12H), 0.57–0.35 (m, 18H). Calculated analysis for $(\text{C}_{40}\text{H}_{58}\text{OS}_3\text{Sn}_2)_n(\%)$: C, 53.92; H, 6.57; O, 1.80; S, 10.78; Sn, 26.94. Actual analysis: C, 54.11; H, 6.59; S, 10.72.

Synthesis of PTBFTDTBT. M1 (0.1550 g, 0.174 mmol) and **M2** (0.1246 g, 0.174 mmol) were dissolved in dry toluene (10 mL) and *N,N*-dimethylformide (2 mL) in a two-necked flask. The solution was flushed with N_2 for 20 min, and then $\text{Pd}(\text{PPh}_3)_4$ (10 mg) as the catalyst was added into the flask. The polymerization reaction was carefully heated to 110 °C, and the reactants were stirred for 24 h at this temperature under a N_2 atmosphere. Then the reaction mixture was cooled to room temperature, poured into 100 mL of methanol and stirred for an hour. Then the crude polymer was further purified by Soxhlet extractions with methanol, hexane and chloroform. The polymer was recovered as a solid from the chloroform fraction by rotary evaporation. Finally, a blue solid was obtained (158 mg, 81% yield).

GPC (THF): $M_n = 42.7$ kDa; $M_w = 142.9$ kDa; PDI = 3.3. Calculated analysis for $(\text{C}_{64}\text{H}_{78}\text{N}_2\text{O}_3\text{S}_6)_n(\%)$: C, 68.91; H, 7.05; N, 2.51; O, 4.31; S, 17.21. Actual analysis (%): C, 67.62; H, 7.01; N, 2.65.

3. Results and discussion

3.1 Synthesis and structural characterization

As shown in Scheme 1, PTBFTDTBT was prepared from **M1** and **M2** by Stille cross-coupling reaction with a yield of 81%, further purification was carried out by continuous extractions with methanol, hexane and chloroform, and the product was recovered from chloroform. The chemical structures of these compounds were verified by NMR (as shown in Fig. S1–S3[†]). The number of aromatic and aliphatic protons estimated from integration of the peaks is generally consistent with the repeating unit of PTBFTDTBT (as shown in Fig. S4[†]). The GPC results (using polystyrene as the standard and THF as eluent) shows that PTBFTDTBT has a M_w value of 143 kDa with a polydispersity index (PDI) of 3.3 (Table 1), both M_n and M_w are much higher than those of PBDTTDTBT (Table 1),^{12a} which indicated that non-symmetric unit-TBF easily forms higher molecular weight copolymers compared to symmetric unit-BDT, as expected. PTBFTDTBT is readily soluble in common organic solvents such as THF, chloroform, chlorobenzene and ODCB. High molecular weight and appropriate solubility are prerequisites for obtaining high-performance PSC.¹¹

3.2 Thermal stability

The thermal property of PTBFTDTBT was investigated using TGA, as shown in Fig. 1. TGA analysis shows that the onset point of the 5% weight loss is *ca.* 318 °C under an inert atmosphere,

Table 1 Polymerization results and thermal data of PTBFTDTBT

Polymer	M_n (kDa)	M_w (kDa)	PDI	Yield (%)	T_d (°C)
PTBFTDTBT	42.7	142.9	3.3	81	318
PBDTTDTBT ^{12a}	16.7	24.9	1.5	66	331

indicating that this polymer's thermal stability is adequate for the fabrication of the devices.

3.3 Optical properties

The optical properties of the conjugated polymer can be acquired from UV-Vis absorption spectra. Fig. 2a shows the UV-Visible absorption spectra of PTBFTDTBT in chloroform solution and as a thin film cast from chloroform solution on a quartz substrate, and all the related absorption data are listed in Table 2, and the related data from PBDTTDTBT has also been listed for comparison. PTBFTDTBT exhibited a broad absorption from 300 nm to 700 nm, both in solution and as a film. In solution, one absorption band, from 300 nm to 500 nm, has two peaks at around 350 nm and 430 nm, which correspond to the π - π^* transition of their conjugated backbone; the other absorption band, from 500 nm to 700 nm, with a peak at around 580 nm, can be attributed to the intermolecular charge transfer (ICT) absorption.¹⁴ Compared to their absorption in solution, the absorption band of PTBFTDTBT in film was red-shifted; the absorption edge was 761 nm in film, corresponding to the optical bandgap (E_g^{opt}) of 1.63 eV. The absorption peak of PTBFTDTBT as a film (608 nm) is slightly red-shifted, by 23 nm, compared to the peak for PTBFTDTBT in solution (585 nm). More interestingly, a strong absorption shoulder peak at 640 nm emerged in the spectra of PTBFTDTBT as a thin film because of strong intermolecular π - π stacking.¹⁵

In order to further explore the absorption of PTBFTDTBT and PBDTTDTBT, absorption coefficients of the PTBFTDTBT and PBDTTDTBT films on ITO substrate, spin-coating from ODCB solution, are shown in Fig. 2b. It is observed that PTBFTDTBT film has an increased absorption coefficient and slightly red-shifted absorption compared to that of PBDTTDTBT

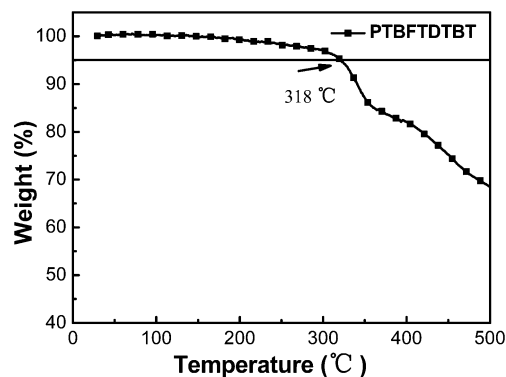


Fig. 1 TGA plot of PTBFTDTBT with a heating rate of 10 K min^{-1} under an inert atmosphere.

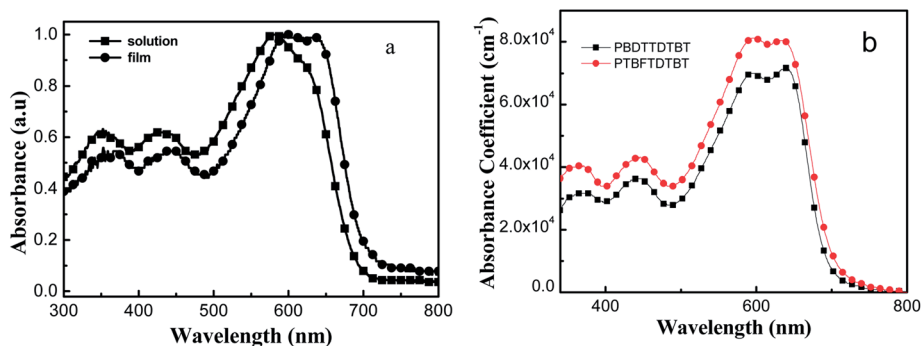


Fig. 2 (a) UV-Vis absorption spectra of PTBFTDTBT in dilute chloroform and as a film on quartz cast from chloroform solution; (b) absorption coefficient spectra of the spin-coated PTBFTDTBT and PBDTTDTBT films on an ITO substrate.

Table 2 Optical and electrochemical properties of PTBFTDTBT and PBDTTDTBT

Polymer	Absorption spectra				Cyclic voltammetry (vs. Ag/AgCl)	
	Sol ^a		Film ^b		p-doping	n-doping
	λ_{\max} (nm)	λ_{\max} (nm)	λ_{onset} (nm)	$E_g^{\text{opt } c}$ (eV)	$E_{\text{ox}}/\text{HOMO}^d$ (V)/(eV)	LUMO ^d (eV)
PTBFTDTBT	585	608	761	1.63	0.80/−5.20	−3.57
PBDTTDTBT ^{12a}	583	640	748	1.66	−/−5.15	−/−3.3

^a Measured in chloroform solution. ^b Cast from chloroform solution. ^c Bandgap estimated from the onset wavelength of the optical absorption.

^d $E_{\text{HOMO}} = -e(E_{\text{ox}} + 4.4)$ (eV); $E_{\text{LUMO}} = E_g + E_{\text{HOMO}}$ (eV) using Ag/AgCl as the reference electrode.

film, which might originate from the higher molecular weight of the regiorandom copolymer PTBFTDTBT – a similar phenomenon has been reported previously.^{11g} The increased absorption coefficient and red-shifted absorption should result in better harvesting of the solar photon flux, thus effectively leading to improved external quantum efficiency (EQE).^{11b,c,e}

3.4 Electrochemical properties

In order to insightfully investigate the electronic properties of the copolymer, CV was carried out (results shown in Fig. 3) to estimate the HOMO level of PTBFTDTBT.¹⁶ The HOMO value for PTBFTDTBT was calculated from the onset of oxidation which was then converted to a potential *versus* saturated calomel electrode (SCE), based on -4.4 eV SCE energy level relative to the vacuum using $E_{\text{HOMO}} = -e(E_{\text{ox}} + 4.4)$ (eV);^{16b} thus, the lowest unoccupied molecular orbital (LUMO) level could be calculated according to $E_{\text{LUMO}} = E_g + E_{\text{HOMO}}$ (eV).¹⁷ Fig. 3 reveals that in a positive potential region, the oxidation is quasi-reversible; the onset oxidation potential (E_{ox}) is 0.80 V, corresponding to a HOMO level of -5.20 eV, which is slightly deeper than PBDTTDTBT, and which is probably because of the stronger electronegativity of the oxygen atom compared to that of the sulfur atoms.¹⁸ PTBFTDTBT has a relatively deep HOMO level, which is beneficial for obtaining high V_{oc} . The LUMO level was calculated to be -3.57 eV using the HOMO level and the optical bandgap. The LUMO energy level of PTBFTDTBT is positioned over 0.4 eV than that of PC₇₁BM (-4.0 eV, measured under the same conditions), which is enough for charge separation and

transfer.¹⁹ All the related CV data and the HOMO–LUMO energy levels (as shown in Fig. 4) for PTBFTDTBT are summarized in Table 2.

3.5 Hole mobility

The charge transport abilities of conjugated polymers have great effects on the photovoltaic properties. Here we measured the hole mobility of PTBFTDTBT using OFET and SCLC methods. As shown in Fig. S5(a) and (b),[†] the typical transfer and output curves of PTBFTDTBT by modulating white light with various intensities were measured by the OFET method. The devices exhibited a moderate p-type field-effect transistor (FET) behavior, as well as having good linear and saturation characteristics. The average hole mobility of PTBFTDTBT is $2 \times 10^{-3} \text{ cm}^2 \text{ V}^{-1} \text{ s}^{-1}$ among six devices. The active layer was annealed at 150 °C for 10 min, and this increased the hole mobility up to $1.53 \times 10^{-2} \text{ cm}^2 \text{ V}^{-1} \text{ s}^{-1}$ as shown in Fig. 5(a) and (b), which may mean that thermal annealing is beneficial to molecular ordering.

The hole mobility of PBFTDTBT was also measured with the SCLC model, which is based on the Poole–Frenkel law using a device structure of ITO/PEDOT:PSS/PTBFTDTBT:PC₇₁BM (1 : 2, w/w)/Au.²⁰ The results are plotted as $\ln(Jd^3/V^2)$ vs. $(V/d)^{0.5}$, as shown in Fig. 5(c). Here, J is current density, d is the thickness of the device, and $V = V_{\text{appl}} - V_{\text{bi}}$, where V_{appl} is the applied potential and V_{bi} is the built-in potential. The SCLC model can be described by the equation:

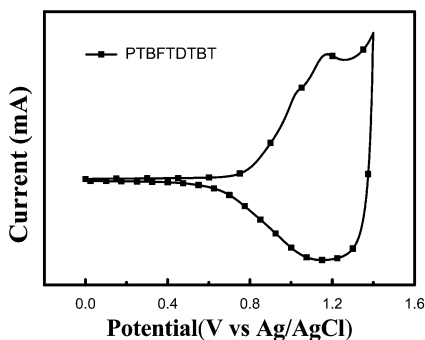


Fig. 3 Cyclic voltammogram of PTBFTDTBT film on a glassy carbon electrode in 0.1 mol L⁻¹ Bu₄NPF₆, CH₃CN solution at a scan rate of 50 mV s⁻¹.

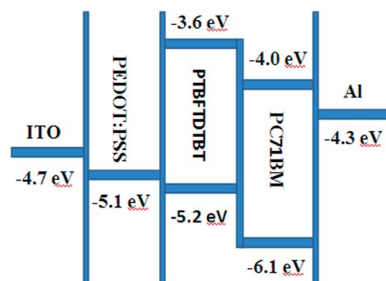


Fig. 4 Energy levels of a PTBFTDTBT-based single junction device.

$$J_{\text{SCLC}} = \frac{9}{8} \epsilon_0 \epsilon_r \mu_0 \frac{(V - V_{\text{bi}})}{d^3} \exp \left[0.89 \gamma \sqrt{\frac{(V - V_{\text{bi}})}{d}} \right] \quad (1)$$

According to eqn (1) and Fig. 5(c), the hole mobility of the blend can be calculated to be $8.3 \times 10^{-2} \text{ cm}^2 \text{ V}^{-1} \text{ s}^{-1}$. Usually a higher molecular weight results in increased hole mobility;^{11g} however, PTBFTDTBT showed a slightly reduced mobility compared to that of its analogue – PBDTDTBT. The slightly reduced mobility probably originated from the regiorandom structure.

3.6 Photovoltaic properties

To investigate the photovoltaic properties of PTBFTDTBT, PSC with a device structure of ITO/PEDOT:PSS/PTBFTDTBT:PC₇₁BM/Ca/Al were fabricated. The active layers were made by spin-casting the blend of PTBFTDTBT and PCBM from ODCB solution, with different weight ratios. Fig. 6 shows the *J-V* curves of the devices under the illumination of AM1.5G, 100 mW cm⁻². The corresponding open-circuit voltage (*V*_{oc}), short circuit current (*J*_{sc}), fill factor (FF) and PCE are presented in Table 3. From the photovoltaic results, we can see that all of the devices show excellent photovoltaic properties, with overall efficiencies over 5%. The device using the weight ratio of PTBFTDTBT and phenyl C₆₁ butyric methyl ester (PC₆₁BM) equal to 1 : 2 (w/w) as

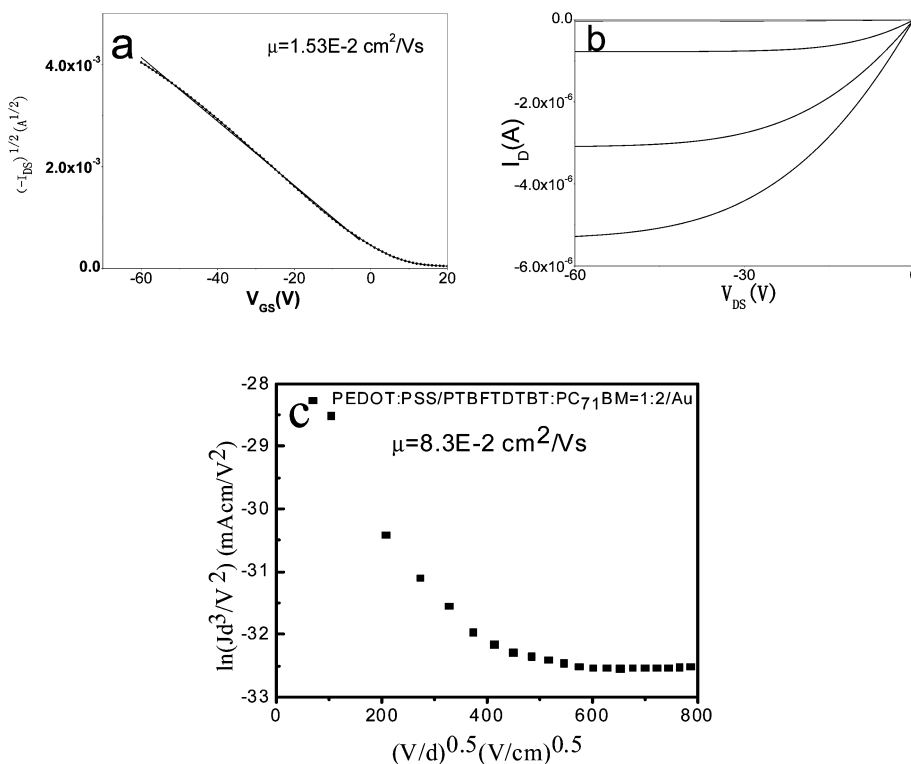


Fig. 5 (a) Transfer characteristics of the PTBFTDTBT annealed at 150 °C for 10 min, measured at *V*_{ds} = -50 V. (b) Output characteristics with *V*_{DS} varying from 10 V to -60 V in steps of 10 V deposited on OTS modified SiO₂. (c) ln(*Jd*³/*V*²) vs. (*V/d*)^{0.5} plot of the PTBFTDTBT/PCBM blend for the hole mobility by the SCLC method.

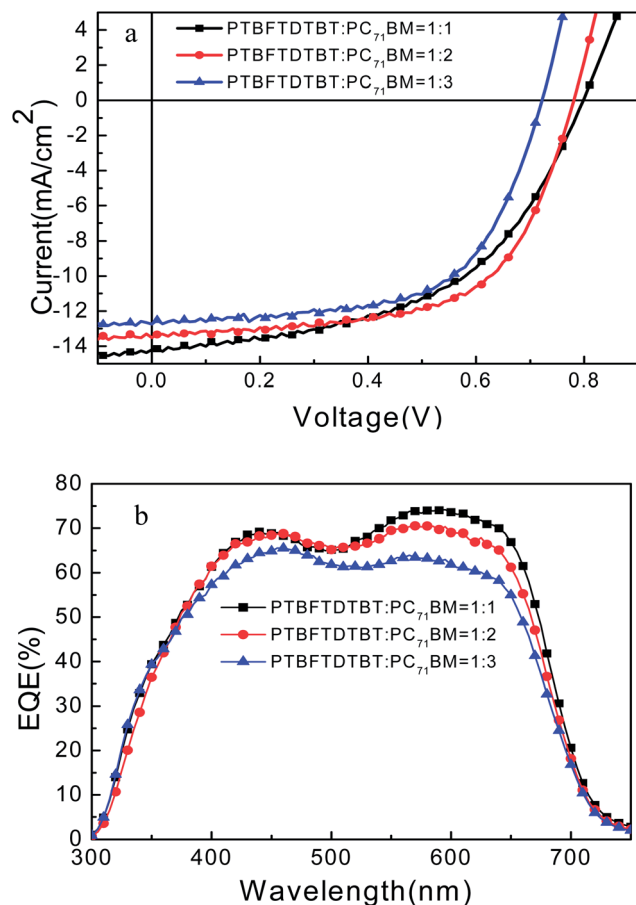


Fig. 6 (a) Typical J - V curves; (b) EQE spectra of polymer solar cells based on PTBFTDTBT and PCBM.

active layer showed the best performance with a PCE of 5.33%, a V_{oc} of 0.79 V, a J_{sc} of 11.64 mA cm⁻² and a FF of 58%. To obtain better photovoltaic properties, PC₇₁BM was used instead of PC₆₁BM blended with PTBFTDTBT as active layer. All of the devices with PTBFTDTBT:PC₇₁BM as the active layer had higher PCE than those with PTBFTDTBT:PC₆₁BM, probably because PC₇₁BM has a broader and stronger absorption spectrum than PC₆₁BM, although it is of similar energy level; therefore, the J_{sc} as well as PCE could be effectively improved

Table 3 Photovoltaic properties of PSC based on PTBFTDTBT:PCBM (different weight ratios, w/w)

Active layer	V_{oc} (V)	J_{sc} (mA cm ⁻²)	FF (%)	PCE (%)
PTBFTDTBT:PC ₆₁ BM = 1 : 1	0.80	11.89	57.4	5.46
PTBFTDTBT:PC ₆₁ BM = 1 : 2	0.79	11.64	58.0	5.33
PTBFTDTBT:PC ₆₁ BM = 1 : 3	0.74	11.21	52.1	5.32
PTBFTDTBT:PC ₇₁ BM = 1 : 1	0.80	14.21	51.4	5.84
PTBFTDTBT:PC ₇₁ BM = 1 : 2	0.78	13.51	61.0	6.42
PTBFTDTBT:PC ₇₁ BM = 1 : 3	0.72	12.74	61.3	5.62
PBDTTDTBT:PC ₇₁ BM = 1 : 1.5 ^{12a}	0.75	10.29	64.0	4.94

with no loss of V_{oc} . Especially when the PTBFTDTBT:PC₇₁BM weight ratio was 1 : 2, the best performance was obtained with a high PCE of 6.42%, a V_{oc} of 0.78 V, a J_{sc} of 13.51 mA cm⁻² and a FF of 0.61. The PSC performance of PTBFTDTBT is much higher than that of PBDTTDTBT, as shown in Table 3, particularly the J_{sc} , which might be mainly because of the higher molecular weight and stronger absorption coefficient of PTBFTDTBT. From the photovoltaic measurement, with the increasing weight ratio of PCBM, V_{oc} showed a decreasing trend; a possible explanation for this phenomenon may be from relatively poor film quality with higher roughness,²¹ as shown in Section 3.7 on morphology.

To verify the PCE of these devices, the EQE spectra of the devices based on the PTBFTDTBT:PC₇₁BM blend as an active layer with different weight ratios (shown in Fig. 6), were investigated. The EQE curves of these devices show a broad wavelength range of 300–750 nm. The calculated photocurrent density of EQE is in accordance with the J_{sc} value measured from the J - V curve, within an experimental error due to the spectral mismatch of the solar simulator.²²

3.7 Morphology

Besides absorption, energy levels and charge mobility, morphology of the active layer is also important for PSC. A suitable morphology is not only beneficial for exciton separation, but is also beneficial for the charge transfer to the respective electrodes and effective charge collection. AFM was carried out to investigate the surface morphology of PTBFTDTBT:PC₇₁BM (1 : 1, 1 : 2, 1 : 3, w/w) blend films spin-coated from an ODCB solution. The resulting height and phase images are shown in Fig. 7. Root mean square roughness (rms) values of the blend films were obtained from AFM images and were found to be 0.77 nm, 0.95 nm and 1.57 nm, for 1 : 1, 1 : 2 and 1 : 3 weight ratios of the PTBFTDTBT:PC₇₁BM blend. From the images, the surface of the PTBFTDTBT:PC₇₁BM (1 : 1, w/w) blend film is quite smooth, with an rms of 0.77 nm. However, when the TEM image was investigated (Fig. S6[†]), this blend film showed polymer spherical domains in some areas with sizes larger than the exciton diffusion length (*ca.* 10 nm), indicating that photogenerated excitons will probably combine before reaching the donor/acceptor (D/A) interfaces, which may lead to relatively lower FF and J_{sc} for the 1 : 1 D/A blend. The blend with the 1 : 3 D/A weight ratio had the highest surface roughness with a less favorable phase separation, which probably explains its relatively low V_{oc} .²¹ For a 1 : 2 D/A weight ratio, the blend showed low roughness and relatively good nanophase separation, as shown in Fig. 7 and S6.† Generally, the nanoscale phase separation can contribute to the formation of a bicontinuous D/A network. Using solvent mixtures or high boiling point solvent additives can usually improve the morphology of the active layer, and probably further assist the formation of a better network to increase the PCE.^{16a,23}

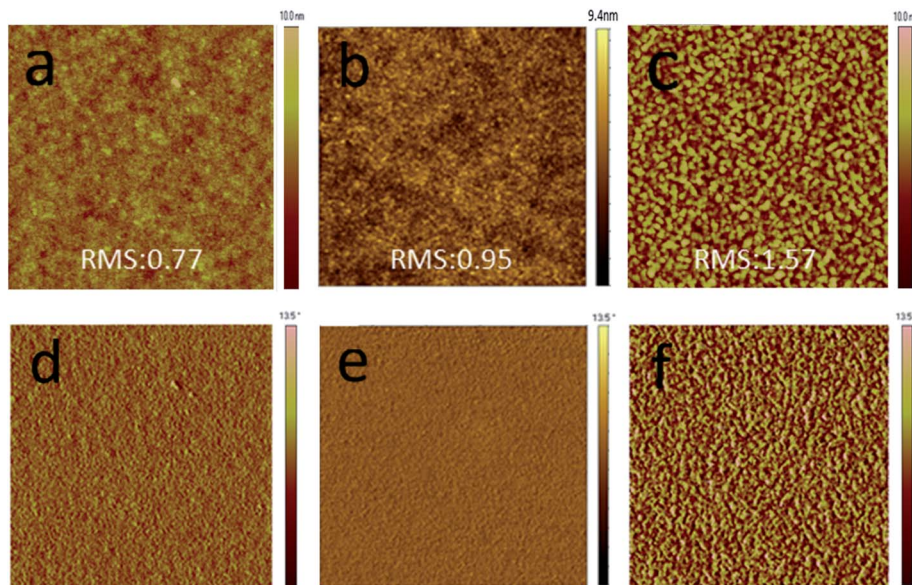


Fig. 7 AFM images (image size: 5 $\mu\text{m} \times 5 \mu\text{m}$) for PTBFTDTBT:PC₇₁BM blend films with different weight ratios spin coated from ODCB: (a–c) height images; (d–f) phase images. PTBFTDTBT:PC₇₁BM blend films with different weight ratios: (a and d) 1 : 1; (b and e) 1 : 2; (c and f) 1 : 3.

4. Conclusions

In conclusion, we changed the hetero atom (O/S) of the polymer backbone, and a new 2D TBF-based polymer (PTBFTDTBT) was designed and synthesized. This small change in the hetero atom (replacing one S in a BDT ring with an O) in the polymer backbone has many advantages, such as increased molecular weight, enhanced absorption coefficient and deeper HOMO level, thus affecting the photovoltaic performance of the solar cells. In this work, the bandgap, photophysical properties and electronic structure of PTBFTDTBT were characterized. PTBFTDTBT exhibited a relatively deep HOMO level of -5.20 eV, a broad absorption and a moderate hole mobility. The PSC based on the blend of PTBFTDTBT and PC₇₁BM (1 : 2, w/w) exhibited the best device performance with a PCE of 6.42%, a V_{oc} of 0.78 V, a J_{sc} of 13.51 mA cm^{-2} and a FF of 61% under illumination of AM1.5G, 100 mW cm^{-2} without any device modifications or post-treatment. These investigations indicate that PTBFTDTBT is a promising donor for PSC.

Acknowledgements

This work was supported by the NSFC (no. 51173206, 21161160443) and National High-Technology Research and Development Program (no. 2011AA050523).

Notes and references

- (a) J. Chen and Y. Cao, *Acc. Chem. Res.*, 2009, **42**, 1709; (b) Y. Li, *Acc. Chem. Res.*, 2012, **45**, 723; (c) Y. Cheng, S. Yang and C. Hsu, *Chem. Rev.*, 2009, **11**, 5868.
- J. You, L. Dou, K. Yoshimura, T. Kato, K. Ohya, T. Moriarty, K. Emery, C. Chen, J. Gao, G. Li and Y. Yang, *Nat. Commun.*, 2013, **4**, 1446.
- (a) J. Bijleveld, A. Zoombelt, S. Mathijssen, M. Wienk, M. Turbiez, D. Leeuw and R. de Janssen, *J. Am. Chem. Soc.*, 2009, **131**, 16616; (b) Y. Liang and L. Yu, *Acc. Chem. Res.*, 2010, **43**, 1227; (c) Y. Liang, Z. Xu, J. Xia, S. Tsai, Y. Wu, G. Li, C. Ray and L. Yu, *Adv. Mater.*, 2010, **22**, 135; (d) L. Huo, Q. Zhang, X. Guo, F. Xu, Y. Li and J. Hou, *Angew. Chem., Int. Ed.*, 2011, **50**, 9697.
- (a) L. Huo, J. Hou, S. Zhang, H. Chen and Y. Yang, *Angew. Chem., Int. Ed.*, 2010, **49**, 1500; (b) Y. Huang, X. Guo, F. Liu, L. Huo, Y. Chen, T. Russell, C. Han, Y. Li and J. Hou, *Adv. Mater.*, 2012, **24**, 3383; (c) L. Dou, J. Gao, E. Richard, J. You, C. Chen, K. Cha, Y. He, G. Li and Y. Yang, *J. Am. Chem. Soc.*, 2012, **134**, 10071; (d) M. Wang, X. Hu, P. Liu, W. Li, X. Gong, F. Huang and Y. Cao, *J. Am. Chem. Soc.*, 2011, **133**, 9638.
- M. Scharber, D. Mühlbacher, M. Koppe, P. Denk, C. Waldauf, A. Heeger and C. Brabec, *Adv. Mater.*, 2006, **18**, 789–794.
- L. Huo, L. Ye, Y. Wu, Z. Li, X. Guo, M. Zhang, S. Zhang and J. Hou, *Macromolecules*, 2012, **45**, 6923–6929.
- B. Liu, B. Qiu, X. Chen, L. Xiao, Y. Li, Y. He, L. Jiang and Y. Zou, *Polym. Chem.*, 2014, DOI: 10.1039/c4py00392f.
- Y. Aeschi, H. Li, Z. Cao, S. Chen, A. Amacher, N. Bieri, B. Özen, J. Hauser, S. Decurtins and S. Tan, *Org. Lett.*, 2013, **15**, 5586.
- J. Hou, H. Chen, S. Zhang, R. Chen, Y. Yang, Y. Wu and G. Li, *J. Am. Chem. Soc.*, 2009, **131**, 15586.
- Z. He, C. Zhong, S. Su, M. Xu, H. Wu and Y. Cao, *Nat. Photonics*, 2012, **6**, 591.
- (a) D. Kim, H. Song, S. Heo, K. Song and D. Moon, *Sol. Energy Mater. Sol. Cells*, 2014, **120**, 94; (b) F. Kim, X. Guo, M. Watson and S. Jenekhe, *Adv. Mater.*, 2010, **22**, 478; (c) M. Tong, S. Cho, J. Rogers, K. Schmidt, B. Hsu, D. Moses, R. Coffin, E. Kramer, G. Bazan and A. Heeger, *Adv. Funct. Mater.*, 2010, **20**, 3959; (d) T. Chu, J. Lu, S. Beaupré, Y. Zhang,

- J. Pouliot, J. Zhou, A. Najari, M. Leclerc and Y. Tao, *Adv. Funct. Mater.*, 2012, **22**, 2345; (e) I. Osaka, M. Saito, H. Mori, T. Koganezawa and K. Takimiya, *Adv. Mater.*, 2012, **24**, 425; (f) W. Li, L. Yang, J. Tumbleston, L. Yan, H. Ade and W. You, *Adv. Mater.*, 2014, DOI: 10.1002/adma.201305251; (g) J. Intemann, K. Yao, H. Yip, Y. Xu, Y. Li, P. Liang, F. Ding, X. Li and A. Jen, *Chem. Mater.*, 2013, **25**, 3188.
- 12 (a) B. Liu, X. Chen, Y. He, Y. Li, X. Xu, L. Xiao, L. Li and Y. Zou, *J. Mater. Chem. A*, 2013, **1**, 570; (b) G. Zuo, Z. Li, M. Zhang, X. Guo, Y. Wu, S. Zhang, B. Peng, W. Wei and J. Hou, *Polym. Chem.*, 2014, **5**, 1976.
- 13 (a) J. Bouffard and T. Swager, *Macromolecules*, 2008, **41**, 5559; (b) R. Qin, W. Li, C. Li, C. Du, C. Veit, H. Schleiermacher, M. Andersson, Z. Bo, Z. Liu, O. Inganäs, U. Wuerfel and F. Zhang, *J. Am. Chem. Soc.*, 2009, **131**, 14612.
- 14 H. Pang, F. Vilela, P. Skabara, J. McDouall, D. Crouch, T. Anthopoulos, D. Bradley, D. de Leeuw, P. Horton and M. Hursthouse, *Adv. Mater.*, 2007, **19**, 4438.
- 15 (a) J. Peet, J. Kim, N. Coates, W. Ma, D. Moses, A. Heeger and G. Bazan, *Nat. Mater.*, 2007, **6**, 497; (b) D. Muhlbacher, M. Scharber, M. Morana, Z. Zhu, D. Waller, R. Gaudiana and C. Brabec, *Adv. Mater.*, 2006, **18**, 2884.
- 16 (a) B. Thompson, Y. Kim and J. Reynolds, *Macromolecules*, 2005, **38**, 5359; (b) Y. Li, Y. Cao, J. Gao, D. Wang, G. Yu and A. Heeger, *Synth. Met.*, 1999, **99**, 243; (c) Q. Peng, X. Liu, Y. Qin, J. Xu, M. Li and L. Dai, *J. Mater. Chem.*, 2011, **21**, 7714.
- 17 W. Lee, S. Son, K. Kim, S. Lee, W. Shin, S. Moon and I. Kang, *Macromolecules*, 2012, **45**, 1303.
- 18 (a) L. Huo, Y. Huang, B. Fan, X. Guo, Y. Jing, M. Zhang, Y. Li and J. Hou, *Chem. Commun.*, 2012, **48**, 3318; (b) X. Chen, B. Liu, Y. Zou, L. Xiao, X. Guo, Y. He and Y. Li, *J. Mater. Chem.*, 2012, **22**, 17724.
- 19 G. Dennler, M. Scharber, T. Ameri, P. Denk, K. Forberich, C. Waldauf and C. Brabec, *Adv. Mater.*, 2008, **20**, 579.
- 20 (a) G. Malliaras, J. Salem, P. Brock and C. Scott, *Phys. Rev. B: Condens. Matter Mater. Phys.*, 1998, **58**, 13411; (b) H. Martens, H. Brom and P. Blom, *Phys. Rev. B: Condens. Matter Mater. Phys.*, 1999, **60**, 8489; (c) Z. Zhang, J. Min, S. Zhang, J. Zhang, M. Zhang and Y. Li, *Chem. Commun.*, 2011, **47**, 9474.
- 21 K. Vandewal, K. Tvingstedt, A. Gadisa, O. Inganäs and J. V. Manca, *Nat. Mater.*, 2009, **8**, 904.
- 22 (a) S. Günes, H. Neugebauer and N. Sariciftci, *Chem. Rev.*, 2007, **107**, 1324; (b) Y. Zou, A. Najari, P. Berrouard, S. Beaupré, B. Aïch, Y. Tao and M. Leclerc, *J. Am. Chem. Soc.*, 2010, **132**, 5330.
- 23 P. Cheng, L. Ye, X. Zhao, J. Hou, Y. Li and X. Zhan, *Energy Environ. Sci.*, 2014, **7**, 1351.